Supplementary Materials

One Cu(I)-I coordination polymer fluorescent chemosensor with amino-rich sites for Nitro aromatic compounds (NACs) detection in water

Yu Zhang [a] , Qingfeng Yang [b], Xiaoping Li [c], Chengxia Miao [a], Qin Hou*[,a], Shiyun Ai *[,a]

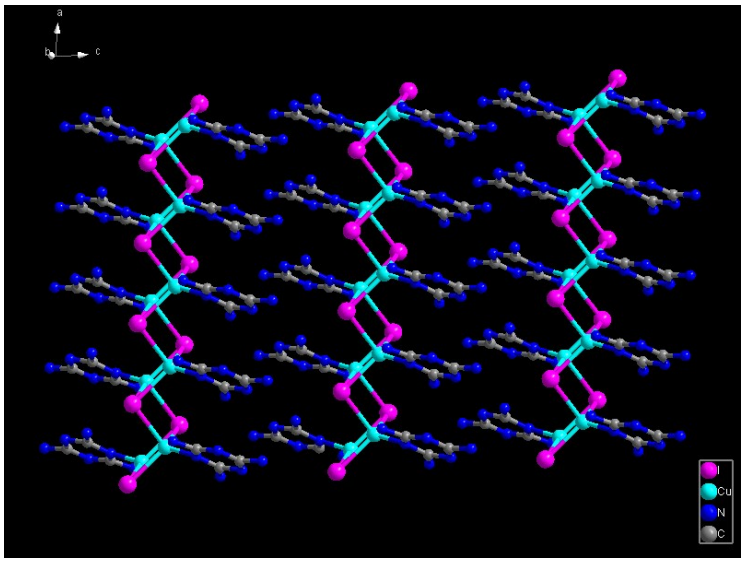

Fig. S1. The stacking graphic of compound **1** in *ac* plane.

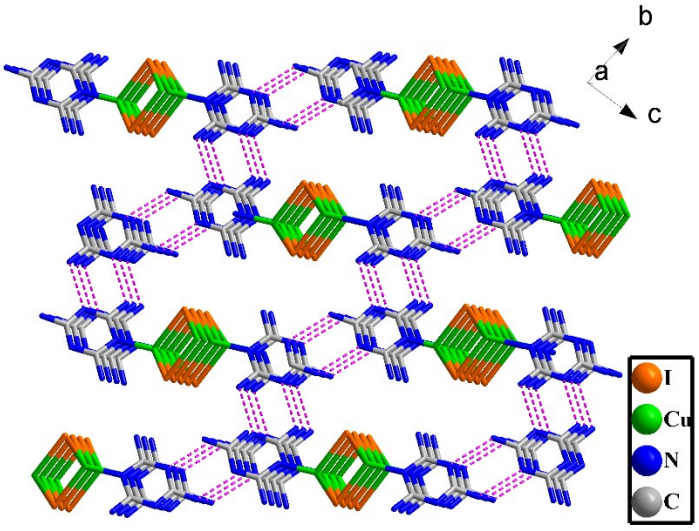

Fig. S2. The 3-D supramolecular architecture of compound **1** in *bc* plane by N (6) -H

(6A)…N (3)#1, N (5) -H (5A)…N (2)#2 H-bonds. Symmetry code: #1 -x, 1-y, 2-z, #2 1-x, 2-y, 2-z.

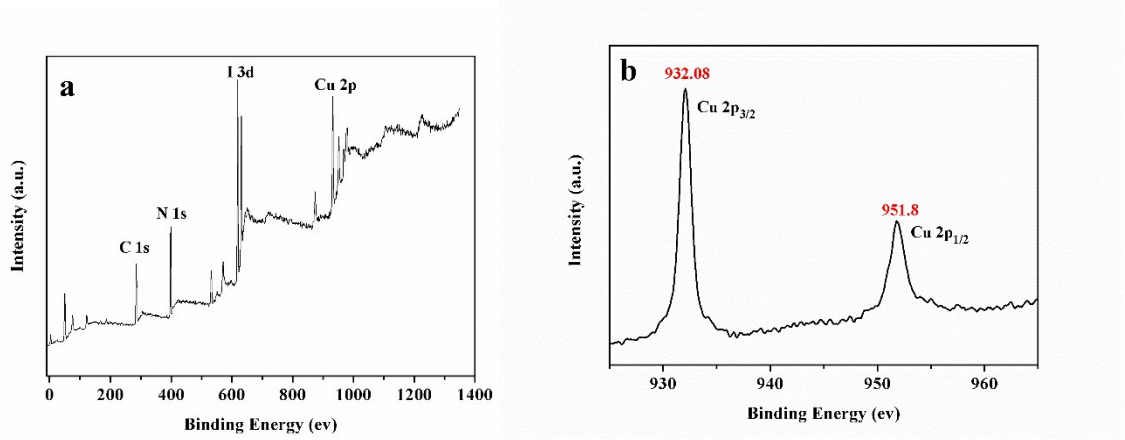

Fig. S3. XPS spectra of compound **1**. (a) survey of **1**, (b) Cu 2p.

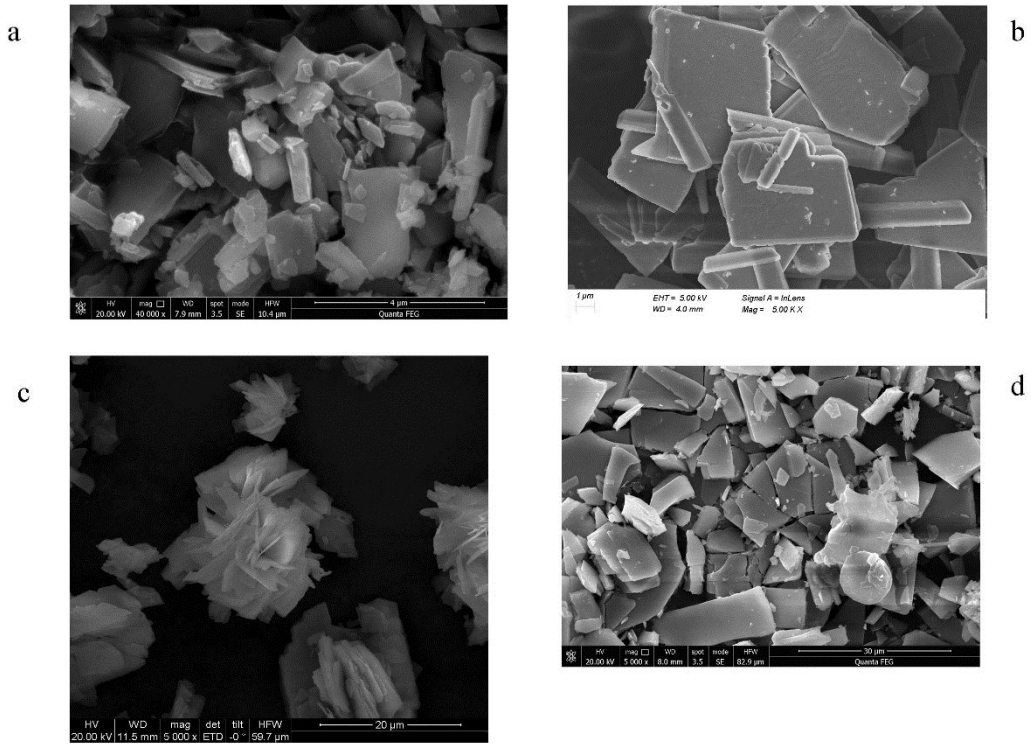

Fig. S4. SEM images nanosheet or nanorod of **1** with different length (~ 2 um for a; ~ 5 um for b; ~ 10 um for c; ~ 15 um for d) and morphologies.

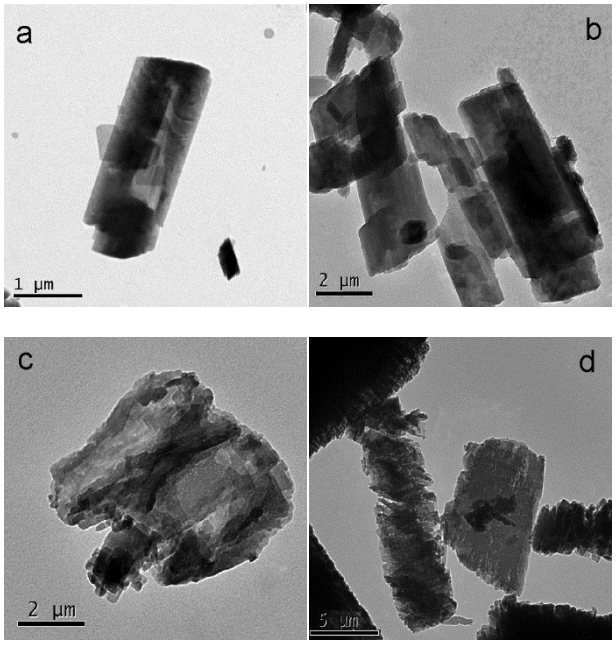

Fig. S5. TEM images nanosheet or nanorod of **1** with different length (~ 2 um for a; ~ 5 um for b; ~ 10 um for c; ~ 15 um for d)

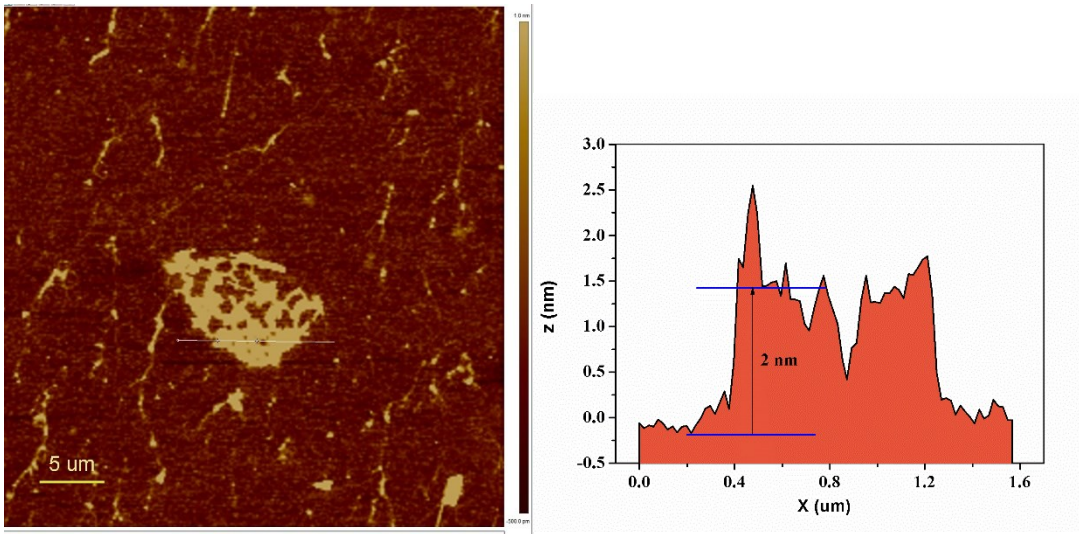

Fig. S6. AFM image of **1** with the length about 10 um and corresponding height profile diagram for the nanosheet.

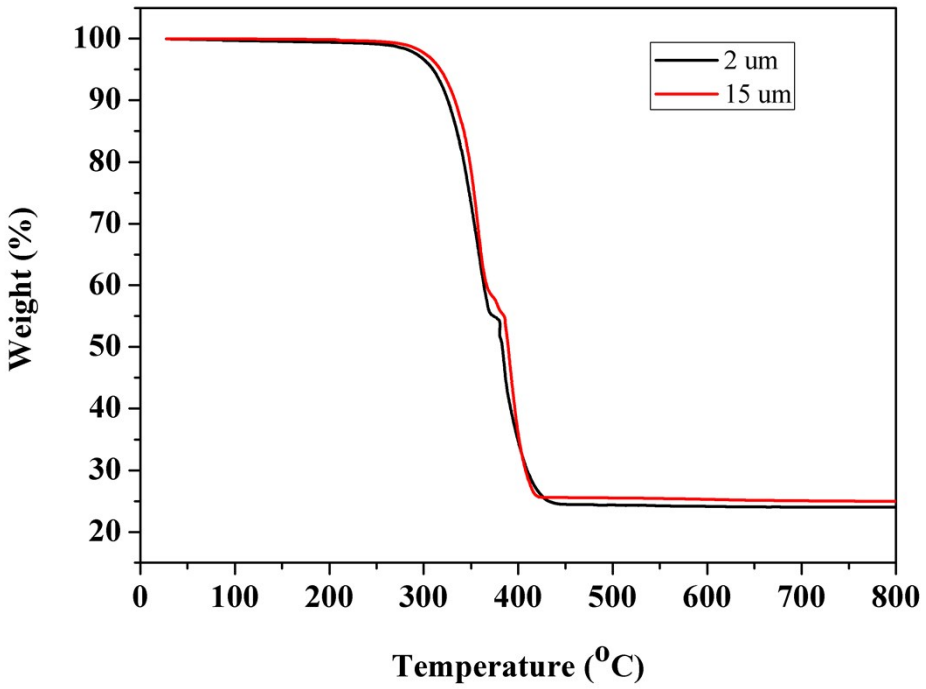

Fig. S7. Thermogravimetric analysis plot for compound **1** with the length of nanosheet (nanorod) about 2 um and 15 um.

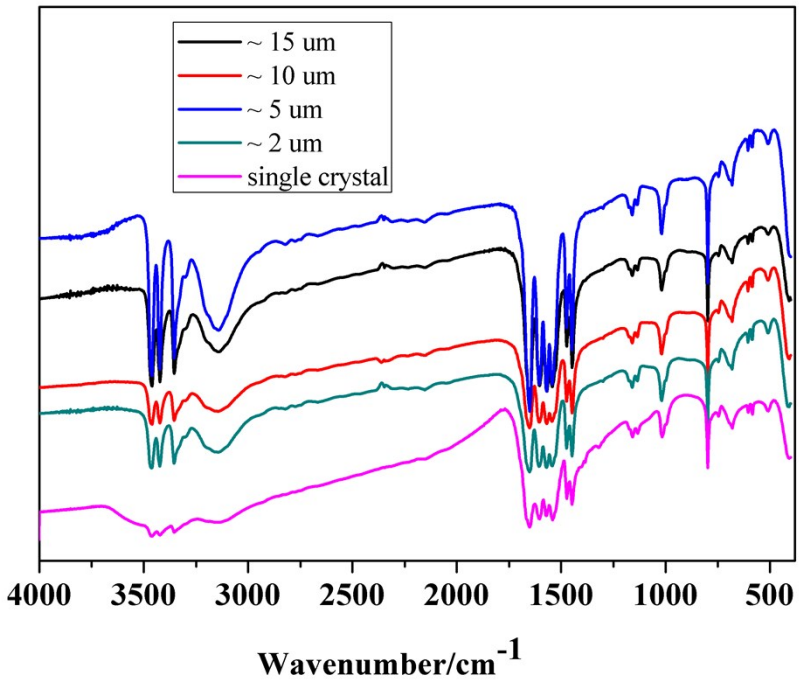

Fig. S8. The IR spectra of compound **1** with single crystal and other different sizes at room temperature.

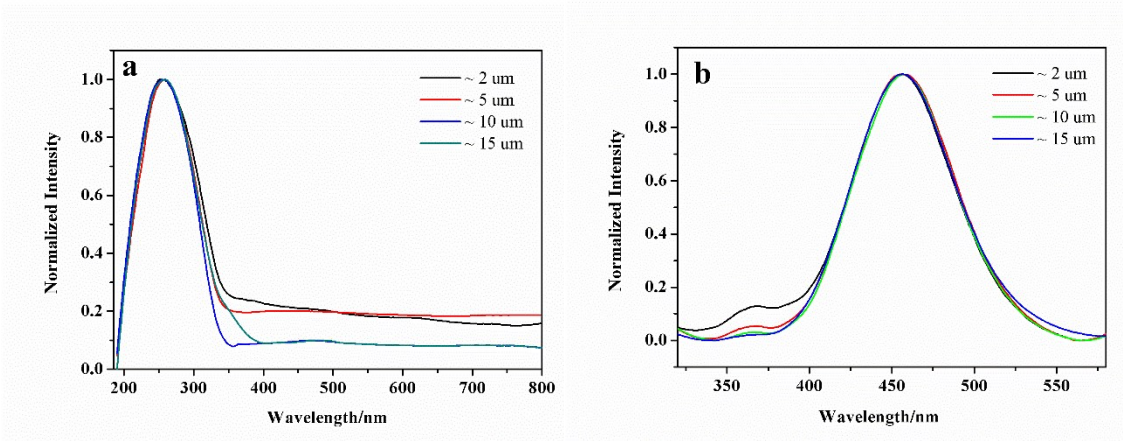

Fig. S9. The solid-state UV-vis spectra (a) and fluorescence emission spectra (b) of compound **1** with different sizes.

Fig. S10. The photograph of compound **1** before and after under irradiation with a UV-vis light at 365 nm.

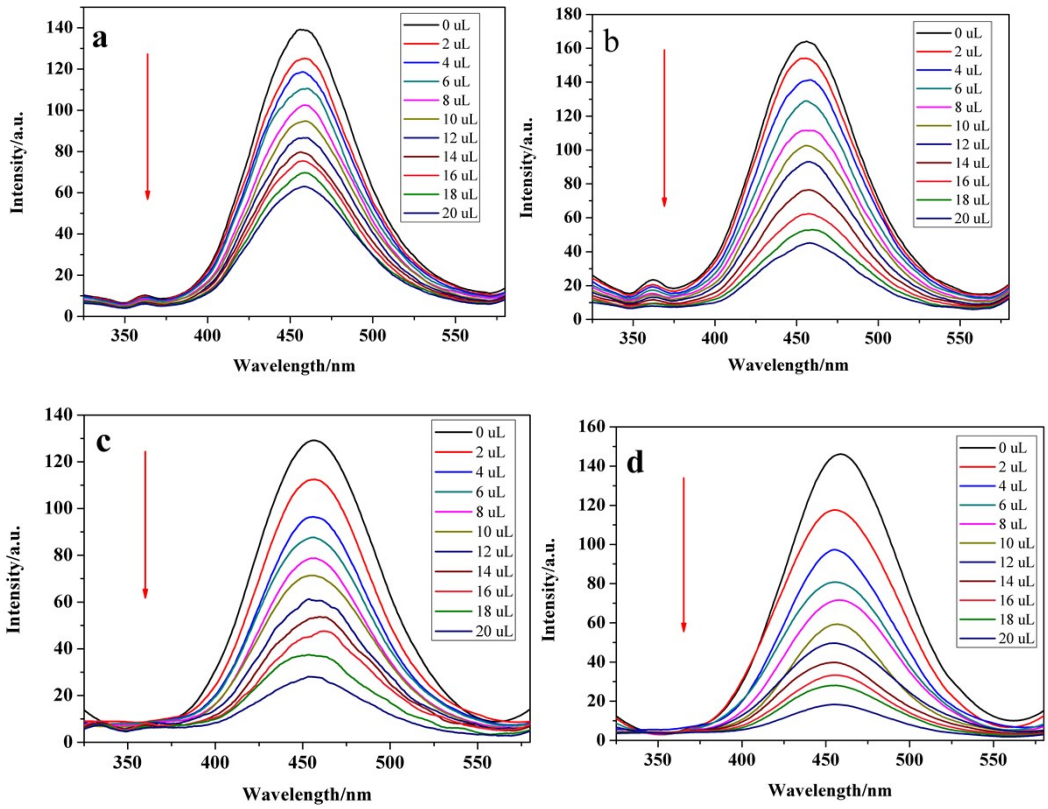

Fig. S11. The emission spectra for different nano scale **1** after addition of TNP (a) ~ 15 um; (b) ~ 10 um; (c) ~ 5 um; (d) ~ 2 um.

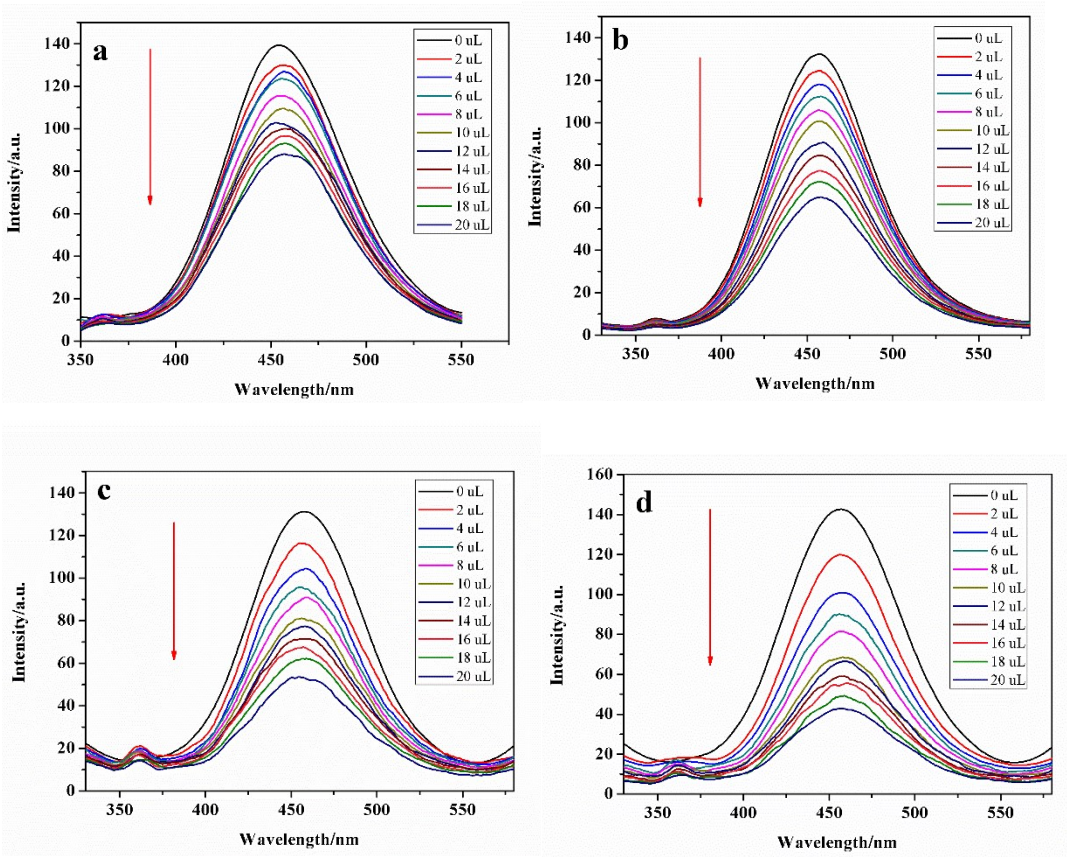

Fig. S12. The emission spectra for different nano scale **1** after addition of 2,4-DNP (a) ~ 15 um; (b) ~ 10 um; (c) ~ 5 um; (d) ~ 2 um.

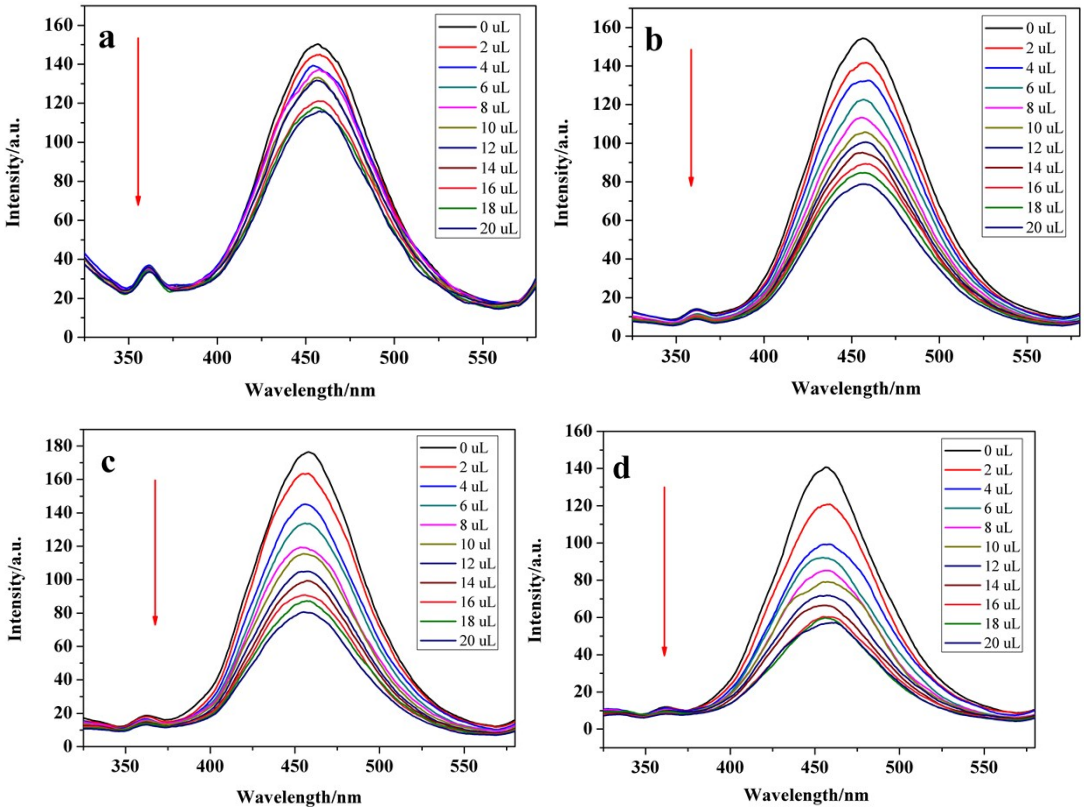

Fig. S13. The emission spectra for different nano scale **1** after addition of 2, 4-DNT (a) ~ 15 um; (b) ~ 10 um; (c) ~ 5 um; (d) ~ 2 um.

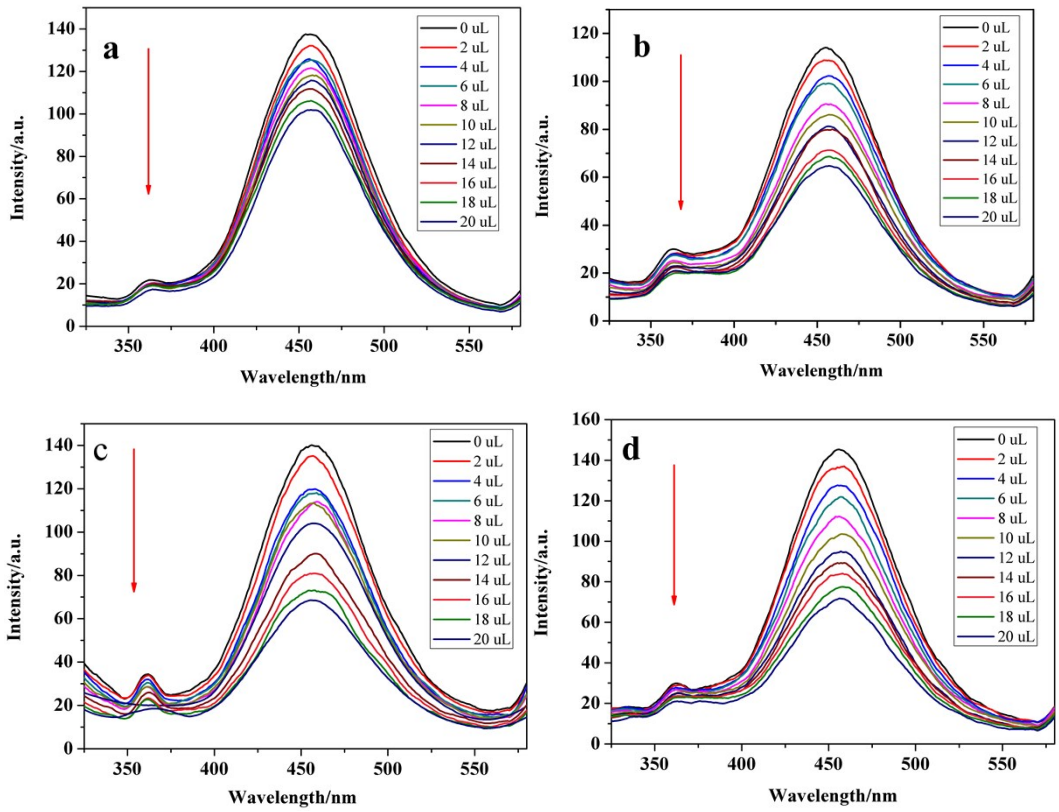

Fig. S14. The emission spectra for different nano scale **1** after addition of 4-NP (a) ~ 15 um; (b) ~ 10 um; (c) ~ 5 um; (d) ~ 2 um.

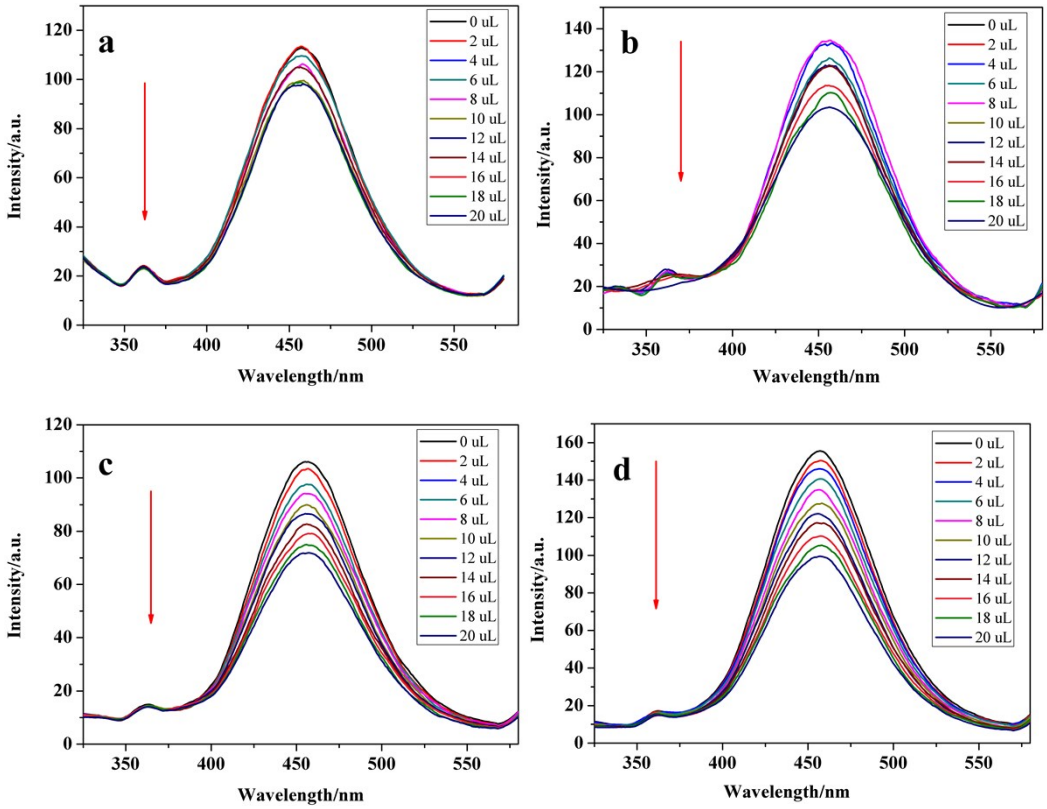

Fig. S15. The emission spectra for different nano scale **1** after addition of NB (a) ~ 15 um; (b) ~ 10 um; (c) ~ 5 um; (d) ~ 2 um.

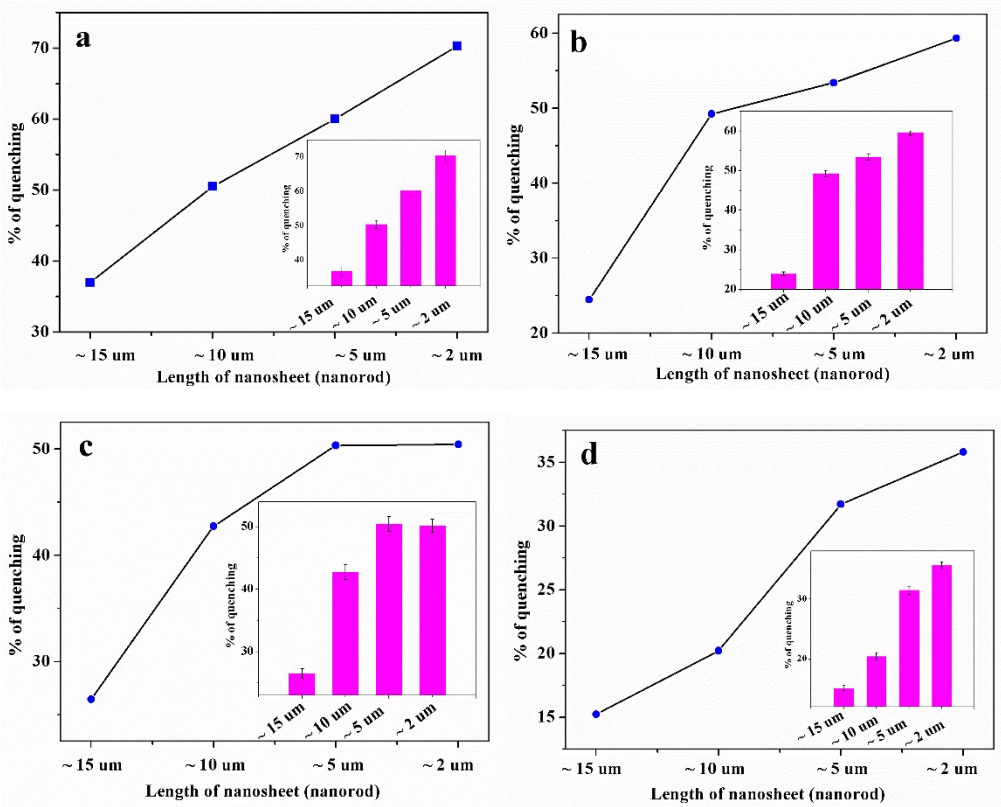

Fig. S16. The plot of quenching efficiency of **1** to 2,4-DNP (a); 2,4-DNT (b); 4-NP (c); NB (d) with different sizes. Inset: the percentage of enhancement of the fluorescence quenching with respect to particle sizes.

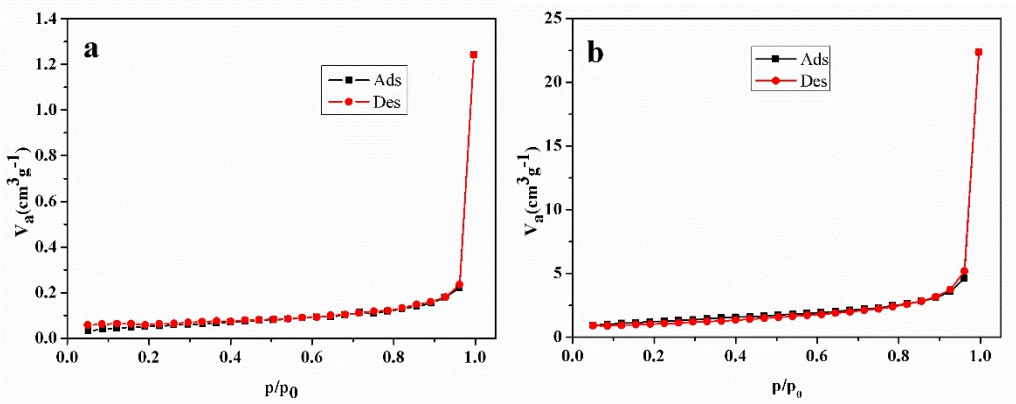

Fig. S17. Adsorption isotherm of N_2 for ~ 15 um sample (a) and ~ 2 um sample. The BET surface area for both samples are 0.198 m^2g^{-1} and 4.249 m^2g^{-1}, respectively.

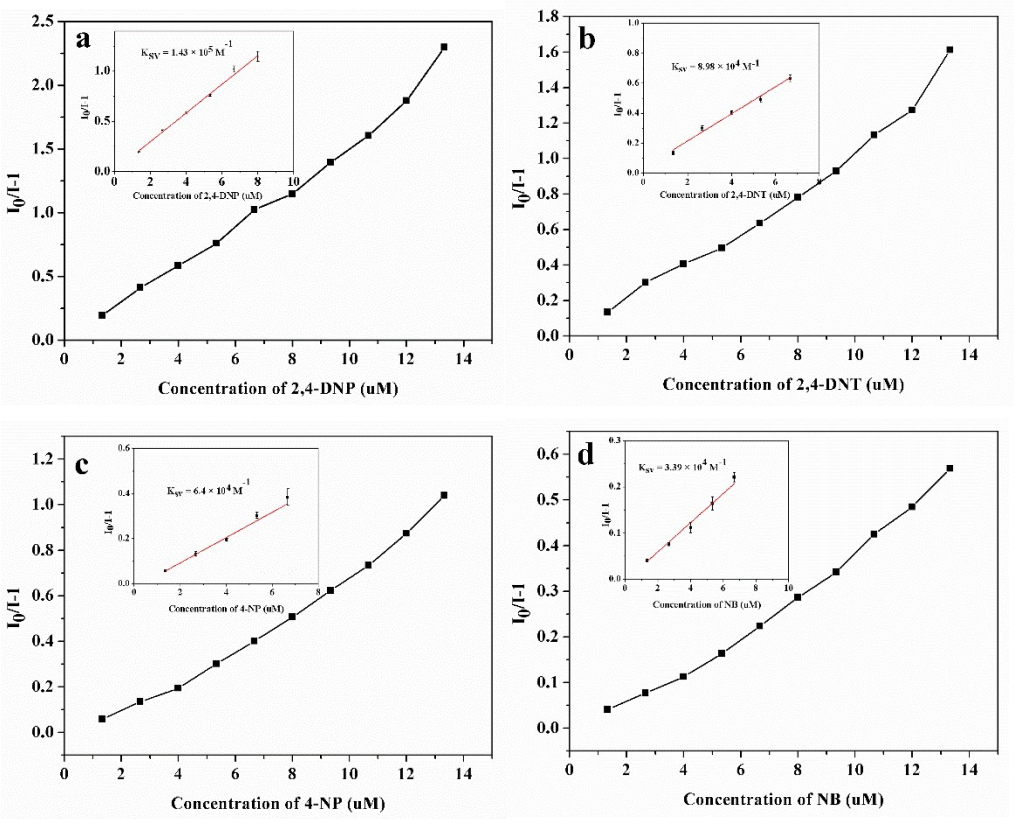

Fig. S18. The SV plot of 2,4-DNP (a); 2,4-DNT (b); 4-NP (c); NB (d) in water suspension of **1**. Insets: linear fitting within the lower concentration region with R^2 = 0.994, 0.984, 0.985, 0.979 for 2,4-DNP, 2,4-DNT, 4-NP and NB, respectively.

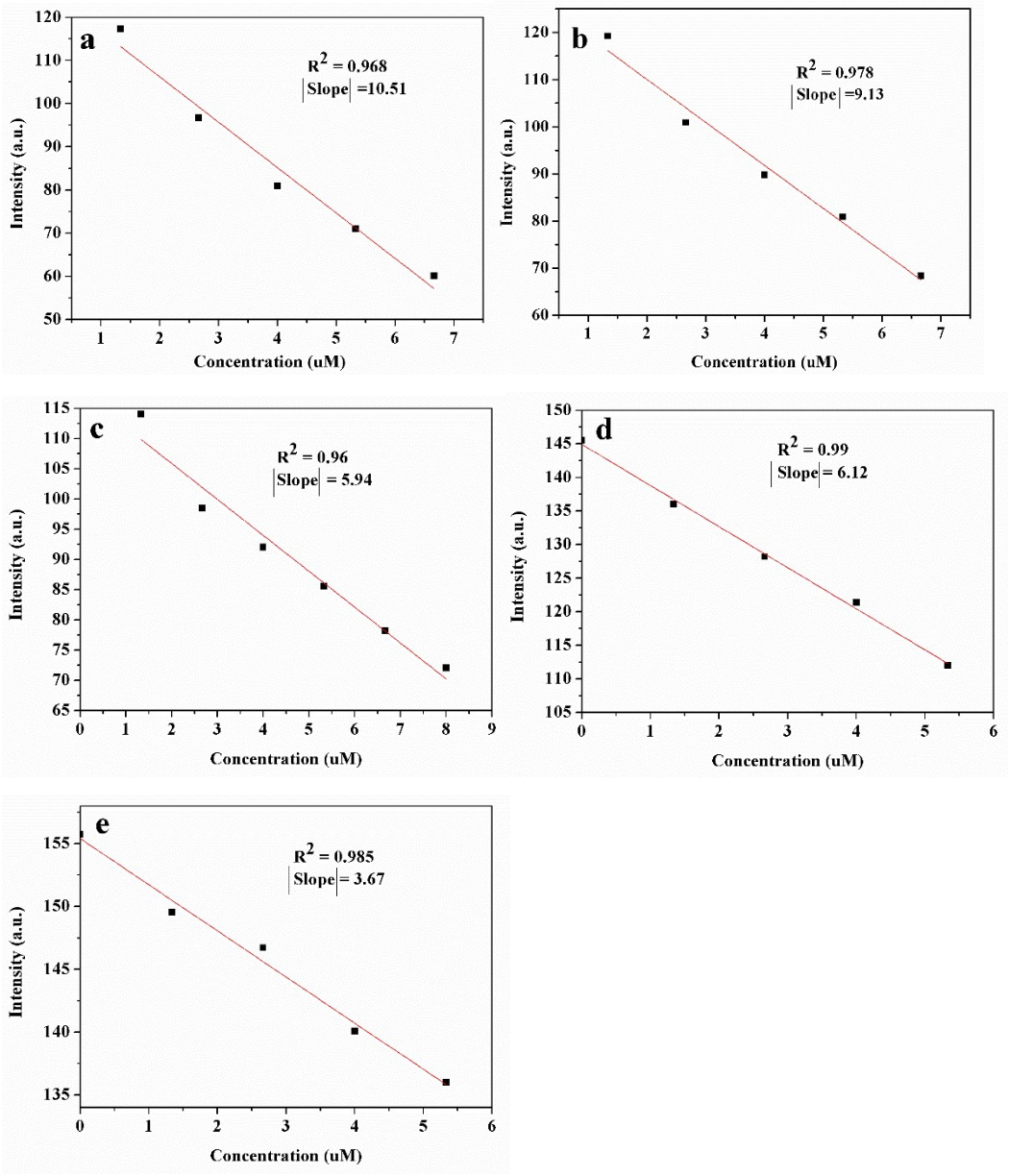

Fig. S19. The intensity vs. concentration plot for TNP (a), 2,4-DNP (b), 2,4-DNT (c), 4-NP (d) and NB (e).

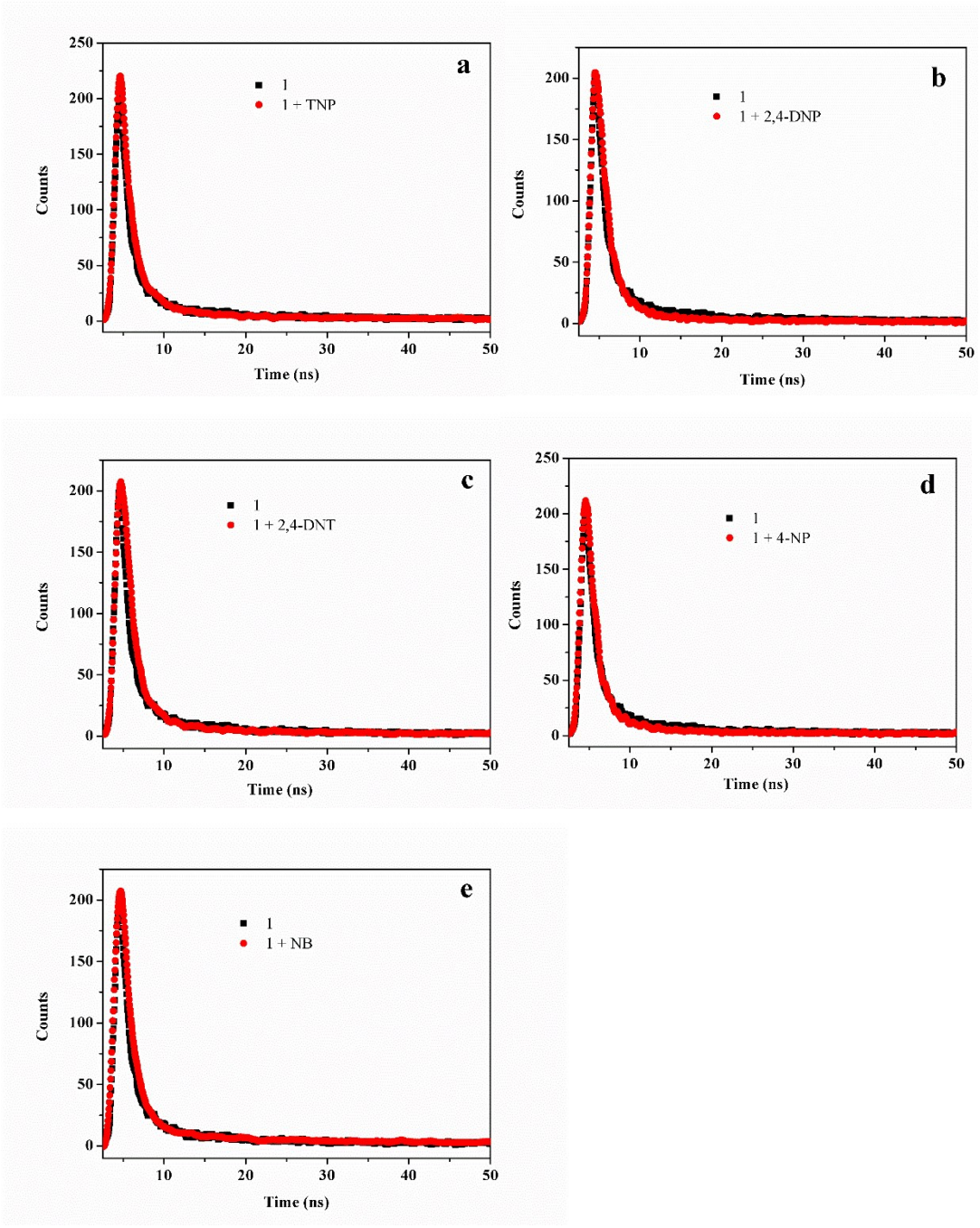

Fig. S20. The fluorescence lifetime of **1** before and after addition of TNP (a); 2,4-DNP (b); 2,4-DNT (c); 4-NP (d); NB (e) (12 uL, 10 mM).

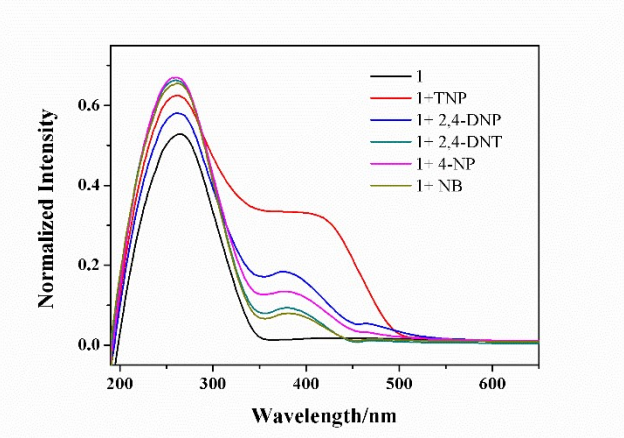

Fig. S21. The solid-state UV-vis spectra of compound **1** and after **1** immersed in NACs.

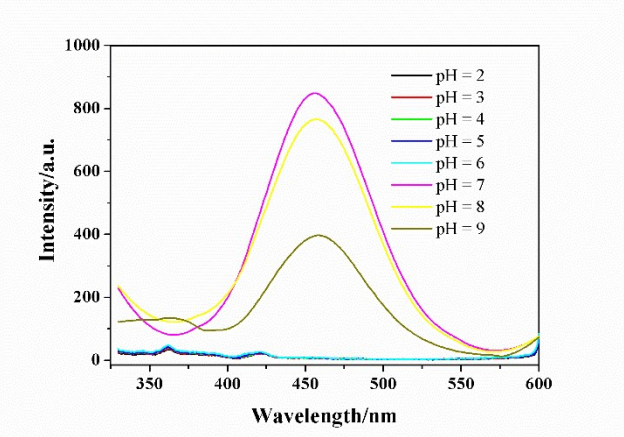

Fig. S22. The effect of pH on the fluorescence emission spectra of compound **1**.

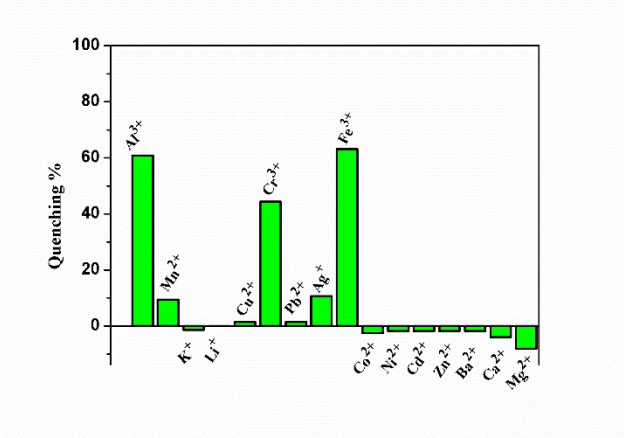

Fig. S23. The fluorescence quenching efficiency of compound **1** by addition of various metal ions (0.025 M).

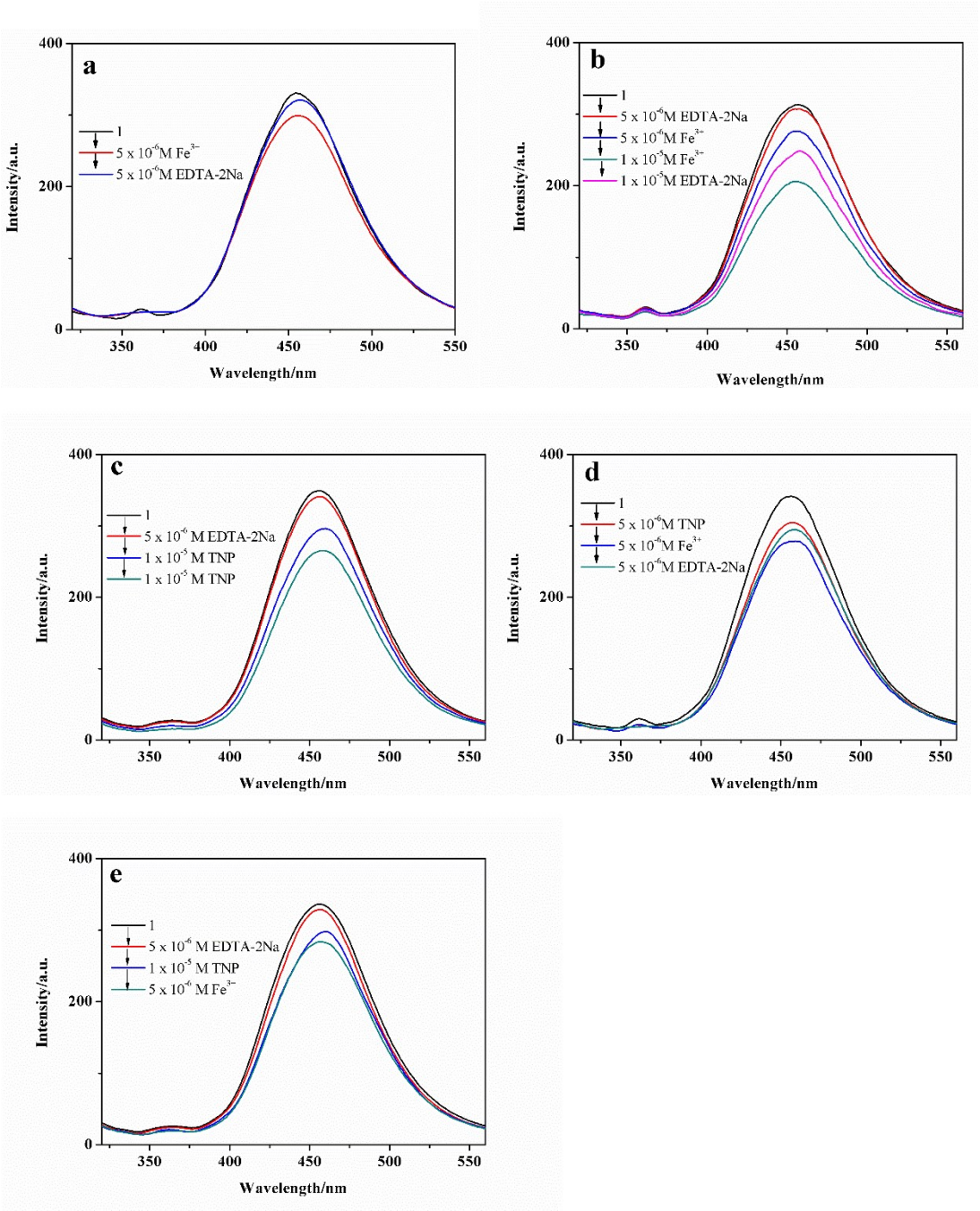

Fig. S24. The change of fluorescence intensity of compound **1** by addition of Fe^{3+} ions before and after addition of EDTA-2Na ((a) and (b)) and the detection of TNP in presence of masking agent (c), (d) and (e).

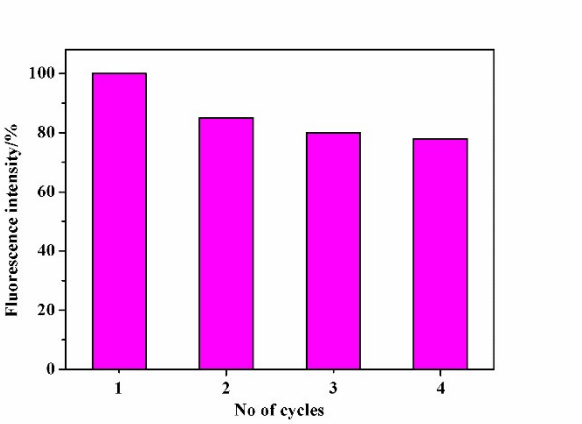

Fig. S25. The changes of emission intensity of **1** after four recycles detection of TNP.

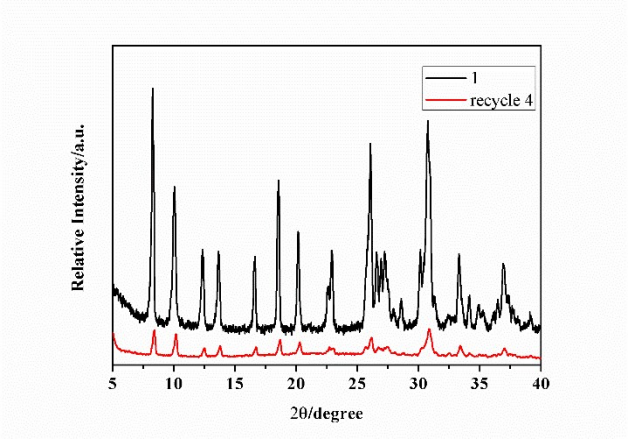

Fig. S26. The PXRD patterns of compound **1** and after four recycles detection of TNP.

Table S1: Synthetic conditions for different sizes of nano scale of **1**.

Size	CuI (mmol)	MA (mmol)	DMF-H_2O (V: V = 1:2) (mL)	EtOH-H_2O (V: V = 1:1) (mL)
~ 15 um	1	1	0	16
~ 10 um	1	1	21	0
~ 5 um	1	1	30	0
~ 2 um	1	1	0	40

Table S2: Crystallographic data for **1**.

Empirical formula	$C_6H_{12}N_{12}I_2Cu_2$ (**1**)
Formula weight	633.16
Space group	triclinic
a/Å	4.0787(3)
b/Å	9.0943(6)
c/Å	10.9148(7)
V/Å^3	387.69(5)
Z	1
*D*c/Mg mm^{-3}	2.712
μ/mm-1	6.740
F(000)	296
Radiation	MoKα (λ = 0.71073)
Reflections collected	2914
Independent reflections	1390 [R_{int} = 0.0332, R_{sigma} = 0.0486]
Data/restraints/parameters	1390/0/103
Goodness-of-fit on F2	1.044
Final R indexes [I>=2σ (I)]	R_1[a] = 0.0259, wR_2[b] = 0.0492
Final R indexes [all data]	R_1 = 0.0299, wR_2 = 0.0521
[a] $R_1 = \Sigma\|\|Fo\| - \|Fc\|\|/\Sigma\|Fo\|$. [b] $wR^2 = \|\Sigma w(\|Fo\|^2 - \|Fc\|^2)^2/\Sigma\|w(Fo^2)^2\|^{1/2}$	

Table S3: Selected bond lengths and bond angles in compound **1**.

	Bond lengths (Å)		Bond angles (degree)
Cu (1)-I (1)	2.6412(7)	I (1)-Cu (1)-I (1) #1	97.765(2)
Cu (1)-I (1) #1	2.7716(8)	I (1)-Cu (1)-I (1) #2	115.465(2)
Cu (1)-I (1) #2	2.7180(7)	I (1) #1-Cu (1)-I (1) #2	92.969(2)
Cu (1)-N (1)	2.018(4)	Cu (1) #4-I (1)-Cu (1) #1	87.031(2)
Cu (1)-Cu (1) #2	2.8619(12)		
Cu (1)-Cu (1) #3	3.7801(3)		

Symmetry transformations used to generate equivalent atoms:

#1 1+x, y, z #2 1-x,1-y, 1-z #3 2-x, 1-y, 1-z #4 x-1, y, z

Calculation of Quantum Yield (Φ)

Quinine sulfate solution (dissolved in 0.5 M H_2SO_4) was taken as the reference for the calculation of the fluorescence quantum yield.

Quantum Yield (Φ) = Φ_R $*I*A_R*\eta^2/I_R*A*\eta_R^2$ (Subscript R is representing the reference Quinine Sulfate)

$\Phi_R = \Phi_{emi} = 0.546$, λ_{emi} =340 nm

A = Optical density.

I = Integrated emission intensity.

η = Refractive index. For H_2O η = 1.333.

All of the photo-physical experiments were carried out in the same experimental condition.

Table S4: Data chart for the Quantum Yield of **1**.

Solution under experiment	**Integrated emission intensity (I)**	**Optical density (A)**	**Quantum yield (Φ)**
Quinine sulfate in 0.5M H_2SO_4	80352	0.0105	0.5460
1	8082	0.033	0.0173

Limit of detection (LOD) calculation

The limit of detection of TNP, 2,4-DNP, 2,4-DNT, 4-NP and NB was calculated using the conventional formula:

$$LOD = 3\sigma/slope$$

Where, the standard deviation (σ) was calculated via the measurement of six successive fluorescence intensity of compound **1** with the nano length of 2 um in absence of NACs (under the same condition). The slope obtained by plotting the emission intensity of compound **1** against the concentration of NACs added.

Table S5: Standard deviation calculation

Blank	Fluorescence intensity
#1	315.3933
#2	315.0562
#3	315.0457
#4	312.3596
#5	309.6292
#6	310.618
Standard deviation (σ)	2.5134

Table S6: LOD calculation.

NACs	σ	|slope|	LOD
TNP	2.5134	10.51	0.717 uM
2,4-DNP	2.5134	9.13	0.826 uM
2,4-DNT	2.5134	5.94	1.269 uM
4-NP	2.5134	6.12	1.232 uM
NB	2.5134	3.67	2.055 uM

Table S7: Comparison of different fluorescent materials used for sensing TNP.

Materials	Media	Analyte	K_{sv} (M^{-1})	sensors	Ref.
1	water	TNP	2.2×10^5	0.03 mg·mL^{-1}	This work
{$Zn_2(tpt)_2(tad)_2\cdot H_2O$}	water	TNP	7.8×10^4	0.08 mg·mL^{-1}	15
$[Zn_8(ad)_4(BPDC)_6O\cdot 2Me_2NH_2]\cdot G$ (G=DMF and water)	water	TNP	4.6×10^4	0.5 mg·mL^{-1}	16
5-((4,6-diamino-1,3,5-triazin-2-yl) amino) isoph-thalic acid (H_2 ATAIA)	water	TNP	1.759×10^5	0.5 mg·mL^{-1}	17
$[NH_2(CH_3)_2][Zn_4O(bpt)_2(bdc)_{0.5}]\cdot 5DMF$	DMF	TNP	1.69×10^4	1 mg·mL^{-1}	39